Catalysis Today 169 (2011) 45–51

Contents lists available at ScienceDirect

Catalysis Today

journal homepage: www.elsevier.com/locate/cattod

Formaldehyde activation by Cu(I) and Ag(I) sites in ZSM-5: ETS-NOCV analysis of charge transfer processes

E. Broclawik[a,*], J. Załucka[b], P. Kozyra[b], M. Mitoraj[b], J. Datka[b]

[a] Institute of Catalysis, Polish Academy of Sciences, ul. Niezapominajek 8, 30-239 Krakow, Poland
[b] Faculty of Chemistry, Jagiellonian University, ul. Ingardena 3, 30-060 Krakow, Poland

ARTICLE INFO

Article history:
Available online 21 September 2010

Keywords:
QM/MM modeling
Cu(I) and Ag(I) sites in MFI
Formaldehyde activation
Electron density transfer channels
ETS-NOCV analysis

ABSTRACT

Adsorption and activation of formaldehyde molecule by copper and silver sites in ZSM-5 was studied by combined QM/MM methodology. ETS-NOCV analysis was applied to decompose the deformation density (the difference between electron densities of composed systems and non-interacting fragments) into independent density flow channels. The analysis disclosed that the bonding of formaldehyde by the metal site may be described in terms of lone pair donation from carbonyl oxygen to the metal and π^*-backdonation from metal d orbitals to antibonding orbital of CO. The former one is responsible for the formation of coordinate bond ("dative covalent") and the latter one for the activation of carbonyl bond. Cu(I) site is more efficient with respect to both processes than Ag(I) one. Zeolitic environment is shown to weaken the bond between formaldehyde and M(I) with respect to free cations for both metals whereas it enhances π^*-backdonation in the case of copper and diminishes π^*-backdonation in the case of silver. Calculated red-shifts of CO frequencies agree well with the IR-measured ones and correlate with the degree of π^*-backdonation which rationalizes as well very good performance of Cu(I) site compared to Ag(I) as the role of zeolitic framework in modifying exchanged cation properties.

1. Introduction

Copper containing zeolites have long drawn strong attention because of their activity in the decomposition of NO (as reported for the first time by Iwamoto, e.g. see Refs. [1,2]). Moreover, Cu^+ exchanged ions in zeolites CuZSM-5, CuX, CuY and CuMCM-41 were found to activate multiple carbon–carbon bonds in alkenes (ethene, propene, butenes [3–6]), ethyne [7,8], and benzene [9,10]. Cu^+ activated also C=O bonds in acetone and formaldehyde [11,12]. The activation was evidenced by measured red-shift of multiple bond stretching by 80–130 cm^{-1} for alkenes, 168 cm^{-1} for ethyne, 16 cm^{-1} for benzene, 38 cm^{-1} for acetone and 56 cm^{-1} for formaldehyde.

Ag^+ ions in zeolites were also reported [13] to activate multiple bonds in organic molecules, however, the effect was smaller than that for Cu^+. The analysis of apparent activity of copper and silver exchanged cations indicated that it depended on as well coinage metal type as on the type of silicalite framework. To rationalize these findings we have already studied the interaction of Cu^+ or Ag^+ ions in zeolites of MFI structure with ethene, ethyne and benzene molecules by theoretical modeling with the focus on the charge transfer processes accompanying adsorption of small hydrocarbon molecules with double bonds [14–18].

Embedded cluster models of Cu(I) and Ag(I) sites in zeolites hosting adsorbed molecules were also successfully modeled by DFT calculations, enriched by new theoretical method for the analysis of charge transfer processes, based on ETS-NOCV scheme, linking the extended transition state (ETS) approach with the natural orbitals for chemical valence (NOCV) method [19–23]. Charge transfer between the fragments, defined either as the ad-molecule interacting with the site or as the cation with bound adsorbate interacting with silicalite framework was considered. ETS-NOCV analysis allowed addressing individual charge transfer channels in ethene and ethyne molecules interacting with Cu(I) or Ag(I) sites in MFI or FAU zeolites in terms of symmetry, donation or back-donation character and energetic importance [18,24]. This gave a possibility not only to visualize and qualitatively assign the character of each contribution (i.e. σ or π), but also provided its energetic share in the bonding. The role of zeolitic framework in promoting site activity was clarified in a joint analysis of complementary pictures of electron density transfer between framework oxygens and the cation, accompanying donation from or backdonation to the molecule. Finally, the differences in catalytic properties of the two coinage metal sites embedded in various types of zeolitic frameworks showed clearly that copper was more efficient than silver concerning as well its intrinsic ability to back-donate electrons as good match with the framework which rationalized its outstanding catalytic activity.

Formaldehyde molecule represents other type of organic ligand, with both the double C=O bond and free electron pair at the oxygen

---

[*] Corresponding author.
E-mail address: broclawi@chemia.uj.edu.pl (E. Broclawik).

0920-5861/$ – see front matter © 2010 Elsevier B.V. All rights reserved.
doi:10.1016/j.cattod.2010.08.020

end. Thus distinct mechanism and geometry of its interaction with Cu^+ and Ag^+ ions from those for alkenes, ethyne and benzene should be expected. Hence, encouraged by previous promising results for ethene and ethyne we decided to study in this work the interaction of formaldehyde with Cu(I) and Ag(I) sites in ZSM-5 with the use of DFT modeling equipped with ETS-NOCV analysis in hope to extract parameters important for the formaldehyde activation.

2. Methodology

2.1. Calculations

In the present computation we have used the method coupling quantum mechanics and molecular mechanics (QM/MM). In this scheme formaldehyde, coinage metal cation and its nearest neighborhood are treated with quantum chemical accuracy while the rest of the framework is treated with less computationally demanding molecular mechanics with periodic boundary conditions (basic unit contains two elementary cells). Turbomole package [25] was applied at QM level and Gulp code [26] in MM part, both linked via QMPot program [27], a variation of QM/MM method designed for zeolites. Density Functional Theory (DFT) was used as QM method with hybrid potential B3LYP [28] for geometry optimization and frequencies, while PBE [29] potential was used for binding energies (defined as a difference between energy of composed system in its equilibrium geometry and the sum of energies of two non-interacting fragments), since we believe that for binding energy PBE potential is closer to experiment [24]. Both potentials were applied with triple zeta basis set. Calculated frequencies were referred to experimental values measured at room temperature. In classical part of calculations core-shell model potential [30] was used with the parameterization from papers by Sauer and Sierka for Si, Al, O and H atoms [31], Nachtigallová et al. for Cu(I) ion [32], and CVFF parameters for Ag [33]. The interactions between formaldehyde molecule and zeolite framework at MM level were represented by electrostatic interactions, with formaldehyde charges: 0.1 on H atoms, −0.38 on O atom and 0.18 on C atom; dispersion interactions with zeolite O atoms were described by Lennard–Jones potential with parameters from Ref. [34]. Formaldehyde binding energy (BE) was calculated as the difference between total energies of bound system and total energies of non-interacting fragments in their optimal geometries. Energetical and orbital properties of the systems (ETS interaction energies and NOCV analysis of deformation densities, *vide infra*) have been obtained from the single point calculation for the QM part in ADF v. 2009.01 [35] (PBE potential). Nalewajski–Mrozek bond orders calculated from two-electron valence indices based on partitioning of ¼ Tr(ΔP^2) [36] were also evaluated in this step.

Additionally, the geometry optimization for the systems composed of a free cation and a formaldehyde molecule has been done by Turbomole with the same computation parameters as it was in the case of QM part described above. These systems, without the zeolite framework, stand for the reference ones; their properties have been obtained analogously to the same systems embedded in zeolite framework.

In the following paragraphs a combined charge energy decomposition scheme, ETS-NOCV, will be presented. In the pure Ziegler–Rauk energy decomposition approach (extended transition state, ETS) [19,20]. The total binding energy between the interacting fragments (ΔE_{int}) is divided into four chemically meaningful components:

$$\Delta E_{\text{int}} = \Delta E_{\text{dist}} + \Delta E_{\text{elstat}} + \Delta E_{\text{Pauli}} + \Delta E_{\text{orb}} \tag{1}$$

The first component, referred to as the distortion term ΔE_{dist}, represents the amount of energy required to promote the separated fragments from their equilibrium geometry to the structure they will take up in the combined molecule. The second term, ΔE_{elstat}, corresponds to the classical electrostatic interaction between the promoted fragments as they are brought to their positions in the final complex. The third term, ΔE_{Pauli}, accounts for the repulsive Pauli interaction between occupied orbitals on the two fragments in the combined complex. Finally, the last term, ΔE_{orb}, represents the stabilizing interactions between the occupied molecular orbitals on one fragment with the unoccupied molecular orbitals of the other fragment as well as mixing of occupied and virtual orbitals within the same fragment (intra-fragment polarization) after the two fragments have been united.

We have recently introduced the natural orbitals for chemical valence (NOCV) [21–23,37–40]. They are defined as the eigenvectors, ψ, that diagonalize deformation density matrix, $\mathbf{\Delta P}$ [21–23],

$$\Delta \mathbf{P}\mathbf{C_i} = \upsilon_i \mathbf{C_i} \tag{2}$$

where $\mathbf{C_i}$ is a vector containing the coefficients expanding ψ_i in the basis of orthogonalized fragment orbitals λ_j as $\psi_i = \sum_j C_{ij}\lambda_j$, and υ_i is the ith eigenvalue. It was shown that deformation density ($\Delta\rho$) can, in the NOCV representation, be expressed as a sum of pairs of complementary orbitals (ψ_{-k}, ψ_k) corresponding to eigenvalues equal in absolute value, but opposite in signs [21–23,41]:

$$\Delta\rho(r) = \sum_{k=1}^{N/2} \upsilon_k[-\psi_{-k}^2(r) + \psi_k^2(r)] = \sum_{k=1}^{N/2} \Delta\rho_k(r) \tag{3}$$

Such "pairing" property is similar to inter-reactant modes defined within the charge sensitivity analysis by Nalewajski et al. [42].

In the combined ETS-NOCV scheme [43,44], the orbital interaction term (ΔE_{orb}) of ETS approach (see Eq. (1)), is expressed in terms of NOCV's as:

$$\Delta E_{\text{orb}} = \sum_{k=1}^{N/2} \upsilon_k[-F_{-k,-k}^{\text{TS}} + F_{k,k}^{\text{TS}}] \tag{4}$$

where $F_{i,i}^{\text{TS}}$ are diagonal Kohn–Sham matrix elements defined over NOCV with respect to the transition state (TS) density (the mid between the density of combined fragments and the final molecule, hence the word transition state). It follows from Eqs. (3) and (4) that for each complementary NOCV pair, representing one contribution to the deformation density $\Delta\rho_k$, one can not only visualize the electron flow channel, $\Delta\rho_k$, but also estimate its contribution to the bond energy, ΔE_k^{orb} [43,44]. Thus, ETS-NOCV provides both qualitative and quantitative characteristics of a chemical bond within one consistent theoretical framework.

2.2. Models

In this work, M7 cluster (cut-off the ZSM-5 framework), the metal cation M(I) and formaldehyde molecule (FA) are treated with quantum chemical accuracy and the rest of the framework is treated by molecular mechanics. M7 cluster is a fragment of ZSM-5 framework containing 6-member ring made of two consolidated 5-member rings. Our model has one Al atom and is electroneutral. To saturate peripheral bonds in the QM part, silicon atoms from the next coordination sphere are replaced by hydrogen atoms. Cu(I) or Ag(I) has been placed in the middle of 6-member ring and the formaldehyde molecule over the cation with the oxygen lone pair pointing at Cu(I) or Ag(I) center (towards the main channel). Fig. 1 shows an example of the two elementary cells containing M7 cluster hosting Cu(I) with adsorbed formaldehyde after optimization. The geometry of Ag(I) system after optimization was

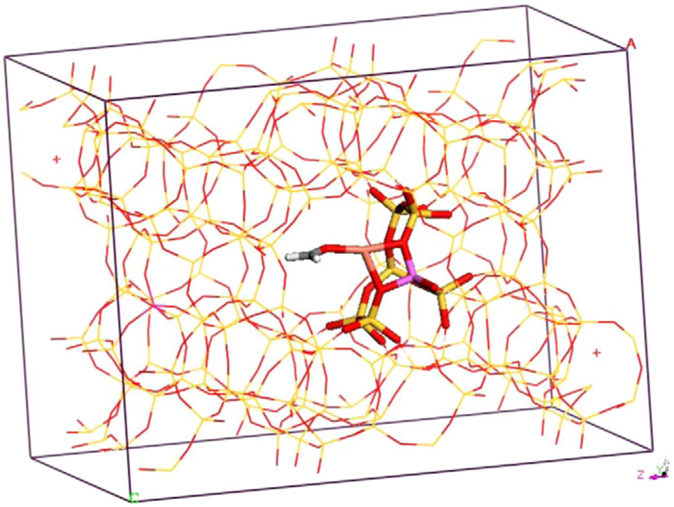

Fig. 1. Periodic element containing Cu(I) cationic site in M7 cluster with adsorbed formaldehyde, embedded in ZSM-5 framework (fragment treated by QM in bold).

qualitatively the same as that for Cu(I) one. In the final geometry, metal cation (with a formaldehyde molecule bound by oxygen atom of carbonyl group) is coordinated only to two oxygen atoms belonging to the same AlO_4 tetrahedron (see Fig. 1), while in the absence of formaldehyde the cations are stronger bound to the framework. The assumed threshold for the Me–O_z bond distance is 2.5 Å. For the unoccupied cationic site the Cu(I) is coordinated by three framework oxygen atoms while Ag(I) cation is coordinated by two framework oxygen atoms within assumed M–O_z bond threshold. Upon formaldehyde adsorption where C=O lone pair ligates the cation, the distances between the cation and framework oxygen atoms increase: the cation becomes withdrawn from the zeolite framework, decreasing coordination to framework oxygens in the case of copper. This indicates that H_2CO molecule bound by oxygen lone pair apparently competes with the zeolite as a ligand. Finally, both cations remain linked with two framework oxygens with the distance to other two of about 4–5 Å.

QM cluster (optimized at QMPot level) was subjected to NOCV analysis in order to extract the information on the electron density rearrangement upon the bond formation. In ADF calculation cluster geometry was not reoptimized since we believe that combined QM/MM calculations better reproduce the structure embedded in zeolite framework than free cluster optimization. In order to analyze electron density transfer processes we apply two types of fragmentation of adsorption system into subsystems. The natural fragmentation of the system composed of an adsorbed molecule (FA) and a site (M7–M(I)) is the one denoted here as [FA]//[M(I)–M7]. This decomposition scheme describes the charge flow between the cationic centre and the molecule. In addition, we consider the alternative partition, denoted as [FA–M(I)]//[M7], where a molecule and a cation stand for one subsystem while a zeolite framework for the other. This partition scheme should bring more specific information on the charge flow between the cation and the zeolite framework. The NOCV method with both partition schemes was described and used previously in the analysis of benzene, ethene and ethyne [16–18] adsorption on Cu(I) and Ag(I) sites in ZSM-5 and ethene interacting with CuY [24]. Additionally, the systems composed of a free cation and a formaldehyde molecule has been subjected to ETS-NOCV analysis within the [FA]//[M^+] partition scheme for the sake of reference.

3. Results and discussion

3.1. Formaldehyde adsorption and carbonyl stretching frequencies

DFT calculations performed in this work for adsorption properties, energetics and carbonyl stretching frequencies indicate that the formaldehyde molecule becomes coordinated by the oxygen lone pair to Cu^+ or Ag^+, as well in the case of free cations as exchanged cations embedded in MFI framework. Typical geometry is shown in Fig. 1 for FA adsorbed on Cu(I)–ZSM-5, the structure of FA adsorbed on Ag(I)–ZSM-5 or free cations differs merely in numerical values of bond distances and bond angles. Table 1 presents important geometrical parameters, binding energies and bond orders for the four adsorption systems considered in this work: $H_2CO–Cu^+$, $H_2CO–Ag^+$, H_2CO–Cu(I)–ZSM-5 and H_2CO–Ag(I)–ZSM-5 (with zeolite represented by M7 cluster embedded in classical force field of MFI framework). Energetic results show that formaldehyde is much stronger coordinated by free cations than by cationic sites in MFI, with the copper always acting as a better site regarding adsorption strength. Framework oxygens act apparently as additional concurring ligands, their lone pairs successfully competing with carbonyl oxygen for electron-accepting center. The bonding between metal cation and carbonyl oxygen becomes weakened by 31.6 kcal/mol for Cu(I) and by 24 kcal/mol for Ag(I) site with respect to free cations. As a consequence, FA becomes rather weakly bound by zeolitic sites which complies with general notion that efficient catalytic sites should not bind prospective substrates very tightly to show good performance.

The same conclusions follow from the inspection of variation in geometric parameters: as well bond distances as bond orders changes indicate that stronger bonds are formed between carbonyl oxygen and bare cations than those with M(I) sites. However, the most important observation concerns the C=O bond weakening (envisaged by the decrease of bond distance and lowering of bond order) that does not follow adsorption strength. In the case of copper, the C=O bond order decrease is larger for Cu(I) site than for Cu^+ whereas in the case of silver zeolitic site is less efficient for C=O bond activation than free Ag^+ cation. This observation shows that the influence of zeolitic environment is opposite for the two coinage metal cations: whereas for Cu^+ embedding in ZSM-5 improves its activation ability with respect to formaldehyde carbonyl group, Ag(I) in ZSM-5 is a worse activator than Ag^+ itself.

On the other hand, the red-shift of C=O IR frequency is a very well-known fingerprint of the bond activation. Table 2 lists the red-shifts of C=O stretching frequency for formaldehyde interacting with bare or embedded Cu^+ and Ag^+ (calculated with respect to gas

Table 1
Selected geometrical and energetic parameters for formaldehyde interacting with four studied systems: bond distances, M–O–C bond angle, binding energy and changes in bond orders (M=Cu, Ag).

	H_2CO	$H_2CO–Cu^+$	$H_2CO–Ag^+$	H_2CO–Cu(I)	H_2CO–Ag(I)
R_{CO} (Å)	1.199	1.221	1.217	1.216	1.210
$R_{M–O_{form}}$ (Å)	*	1.922	2.214	1.884	2.292
$\angle M–O_{form}–C$	*	140.5	139.8	137.0	130.9
BE (kcal/mol)	*	−46.5	−33.7	−14.9	−9.6
$\Delta b.o._{C=O}$	*	−0.23	−0.16	−0.30	−0.11
$b.o._{M–O_{form}}$	*	0.67	0.59	0.44	0.27

Table 2
Red-shits of carbonyl stretching frequencies for formaldehyde interacting with studied systems: calculated values for free or embedded cations and measured IR shifts for M(I)–ZSM-5.

	$\Delta\nu_{CO}$ (cm^{-1})		
	M$^+$	M(I)–M7	Exp.
Cu	−78	−81	−56
Ag	−67	−41	−32
Δ	−11	−40	−24

phase molecule within the same approach). The latter ones have also been registered by IR experiment performed for Cu$^+$ZSM-5 and Ag$^+$ZSM-5 and are listed in the last column [11,12]. Reference values for C=O stretching frequency are 1819 cm^{-1} (calculated) and 1745 cm^{-1} (measured by FTIR experiment). The data presented in Table 2 supply firm evidence for the trends described in the previous paragraph. As well IR experiment as the calculations evidence significant activation of C=O bond in formaldehyde adsorbed on zeolitic cationic sites, with much higher efficiency of Cu(I) than that of Ag(I). The values of carbonyl stretching frequency shifts confirm also positive influence of embedding on Cu(I) and the opposite effect for Ag$^+$ where embedding decreases the C=O red-shift by 26 cm^{-1}. Even if the match between the calculated and measured red-shifts for M(I) sites is not perfect, the role of zeolite framework may be clearly extracted from QM modeling.

3.2. Charge flow processes

The role of charge transfer in the process of adsorption and molecule activation by transition metal sites both in homogeneous and heterogeneous catalysis has long been recognized and discussed in numerous scientific works. Our research on NO and CO molecules as well as on alkenes, alkynes and benzene interacting with Cu(I) and Ag(I) sites in zeolites has already indicated that π^*-backdonation is the decisive factor in multiple bond activation [6,10,14–18,24]. In this contribution we are discussing the results of NOCV analysis in order to pinpoint charge transfer channels important for bonding and activation of formaldehyde.

Fig. 2 presents dominant density transfer channels between the formaldehyde molecule and the other fragment, modeled either as a free Cu$^+$ cation or Cu(I)-M7 cluster. In the case of Cu$^+$ (Fig. 2A) the three distinct channels bring significant contributions to orbital interaction energy and thus to overall binding energy. The first one (with $\Delta E^i_{\text{orb}} = -18.8$ kcal/mol) corresponds to electron pair donation from the carbonyl oxygen to the cation (dative contribution) and the bonding region (covalent part of bonding), these transfer processes will be called LP-donation. It fully conforms to the intuitive picture of a coordinate bond (labeled in the literature as “dative covalent” connection). Due to the fact that during this transfer no density depletes from C=O bonding region, we assume that this term is not meaningful for C=O activation. It should be emphasized that this donative term differs from the corresponding contribution in the case of alkenes and alkynes because in the latter cases the density depletes directly from CC bonding region. The second contribution (with $\Delta E^i_{\text{orb}} = -8.0$ kcal/mol) describes backdonation of electrons from copper d_π orbital to the antibonding π^* orbital of carbonyl. According to our previous findings [18,24] this process was found nearly quantitatively responsible for differences in alkene or alkyne activation on various sites, as it directly leads to the weakening of carbon–carbon bond. The third contribution corresponds to intra-fragment polarization, virtually invariant with the environment and presumably of minor importance for the activation process.

In the case of Cu(I) site (Fig. 2B) the three analogous channels of the charge density transfers follow from differential density decomposition but their share in orbital interaction energy becomes strongly modified by the environment. The role of lone pair donation from carbonyl oxygen is diminished (ΔE^i_{orb} is lowered by 5.5 kcal/mol) whereas the contribution of π^*-backdonation becomes increased by 6.8 kcal/mol. This even reverts the ordering of dominant channels for charge flow making the π^*-backdonation process the most important one as well for the bonding as for the activation of formaldehyde by Cu(I) site. This picture fully goes in line with larger red-shift of C=O stretching frequency calculated for Cu(I)-M7 than that for Cu$^+$. In the case of Ag$^+$ charge transfer channels (Fig. 3A) bring much lower contributions to the orbital interaction energy which complies with the lower orbital interaction and binding energy of formaldehyde than that for Cu$^+$. Only two channels pass the threshold of 1.5 kcal/mol assumed here for meaningful orbital energy contribution: lone pair donation and π^*-backdonation, with the latter one much less significant than that for Cu$^+$ (−4.0 kcal/mol versus −8.0 kcal/mol). Even more interestingly, embedding of Ag$^+$ in ZSM-5 framework diminishes both contributions, with very strong negative impact on π^*-backdonation that becomes nearly negligible for Ag(I) site. This result fully rationalizes somewhat unexpected worsening of Ag(I) activation ability towards carbonyl bond in formaldehyde with respect to the free cation, as observed in modeling and evidenced by much lower C=O IR frequency red-shift registered for Ag(I)–ZSM-5.

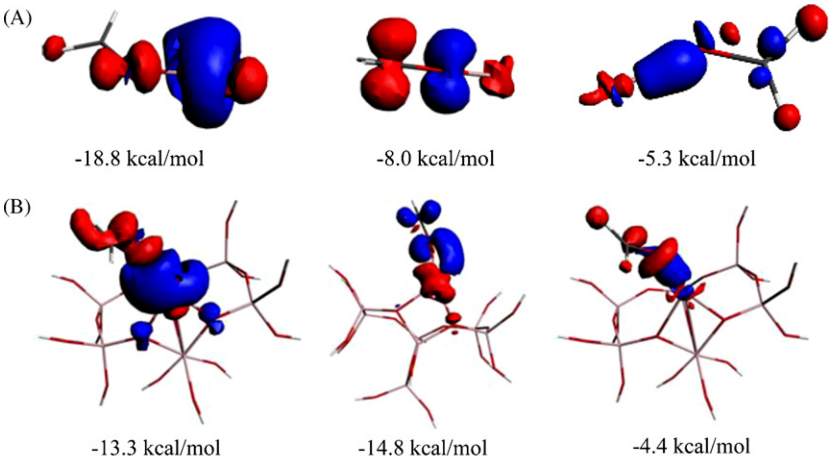

Fig. 2. Dominant contributions to deformation density together with the corresponding energies for [FA]//[Cu$^+$] fragmentation (A) and [FA]//[Cu(I)–M7] fragmentation (B); red-density outflow, blue-density inflow (contour value 0.001 a.u.). (For interpretation of the references to color in this figure legend, the reader is referred to the web version of the article.)

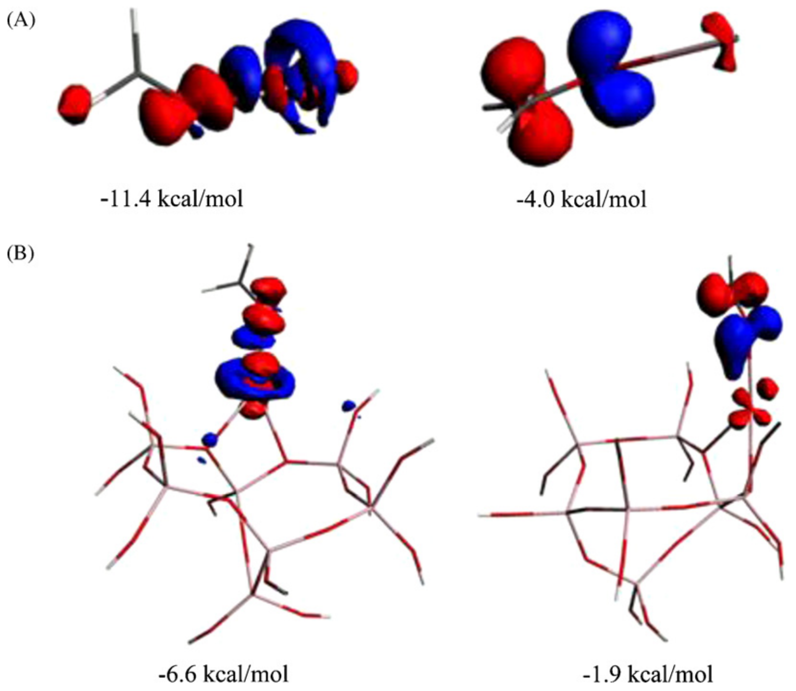

Fig. 3. Dominant contributions to deformation density together with the corresponding energies for [FA]//[Ag$^+$] fragmentation (A) and [FA]//[Ag(I)–M7] fragmentation (B); red-density outflow, blue-density inflow (contour value 0.001 a.u.). (For interpretation of the references to color in this figure legend, the reader is referred to the web version of the article.)

Table 3
Binding energy (BE) and Ziegler–Rauk energy decomposition results for [FA]//[M$^+$:M(I)–M7] fragmentation, together with dominant orbital energy contributions according to ETS-NOCV analysis (all values in kcal/mol).

FA-bound fragment	Copper		Silver	
	Cu$^+$	Cu(I)–M7	Ag$^+$	Ag(I)–M7
BE	−46.5	−14.9	−33.6	−9.6
ΔE_{Pauli}	49.8	61.4	32.0	28.3
ΔE_{elstat}	−57.9	−55.0	−39.4	−28.0
ΔE_{orb}	−39.0	−35.7	−21.4	−12.4
$\Delta E^{i}_{\text{orb}}$				
LP-donation	−18.8	−13.3	−11.4	−6.6
π*-Backdonation	−8.0	−14.8	−4.0	−1.9
Polarization	−5.3	−4.4	–	–

Table 3 collects numerical data for the observations sketched already in preceding paragraphs. ΔE_{orb} values correspond solely to orbital interactions in the ligand binding by the metal site. Moreover, the energy component corresponding to the fragment distortion upon forming bound system (present in BE calculated independently) is not accounted for in ETS-NOCV analysis since fragment geometries were not optimized separately due to the lack of embedding in the energy decomposition step. There is no simple relation between ligand binding energy and orbital interaction, however, there seems to exist firm consensus that no simple relation between adsorption energy and substrate activation should be expected either. Our results of ETS-NOCV analysis indicate that carbonyl bond activation correlates well with selected electronic components of the interaction with transition metal site: while the overall bonding strength depends as well on carbonyl lone pair donation (intuitive picture of coordination bond) as on π^*-backdonation (similarly to Chatt–Duncanson π^*-complexation mechanism), the degree of carbonyl bond activation seems to depend predominantly on the latter factor.

Indeed, Table 3 shows that ligand bonding strength decreases for Cu(I)–MFI site because of diminished lone pair donation and increasing in Pauli repulsion term, while its activation ability increases due to backdonation, clearly enhanced by embedding in zeolitic environment. In the case of silver, embedding in zeolitic framework diminishes the importance of as well lone pair donation as π^*-backdonation channels, Pauli repulsion term and electrostatic contribution, thus as well the bonding strength as carbonyl bond activation are lowered with respect to the free cation.

Finally, let us directly address the impact of ZSM-5 framework on the properties of exchanged cation. Table 4 and Fig. 4 present the results of NOCV-ETS analysis performed for the second fragmentation pattern, namely the cation with bound formaldehyde treated as one fragment and M7 cluster (representing the environment) as the other one. In the case of copper, the channel describing electron density flow from framework oxygens via d_π orbitals of copper to the carbonyl antibonding orbital (strongly polarized towards the carbon) is energetically dominant. This channel clearly illustrates supporting π^*-backdonation by oxygen lone pairs and thus the activation of C=O bond. The second energetically important channel describes the donation of electron density from framework oxygens towards copper which in turn imposes some reverse flow from copper to carbonyl oxygen. Hereafter, we label this channel “LP

Table 4
Dominant orbital energy contributions for [FA]//[M(I)–M7] partition (in kcal/mol) and their roles for ligand binding and activation.

$\Delta E^{i}_{\text{orb}}$	Role	FA–Cu(I)//M7	FA–Ag(I)//M7
π*-Backdonation support	Ligand binding and activation enhance	−18.0	–
LP concurrence	Ligand binding decrease	−12.0	−12.4

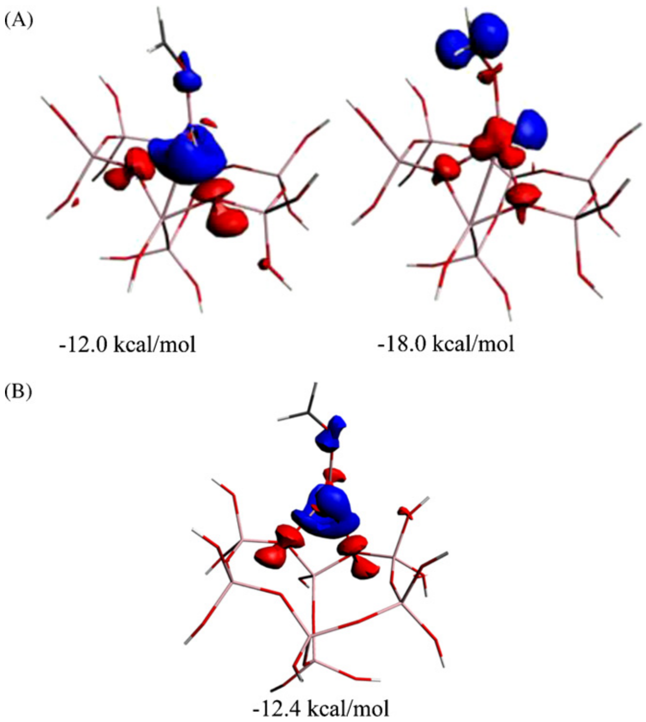

Fig. 4. Dominant contributions to deformation density together with the corresponding energies for [FA–Cu(I)]//[M7] partition (A) and for [FA–Ag(I)]//[M7] partition (B); red-density outflow, blue-density inflow (contour value 0.001 a.u.). (For interpretation of the references to color in this figure legend, the reader is referred to the web version of the article.)

concurrence” and ascribe the weakening of formaldehyde binding energy by M(I) site to this density flow, diminishing dative interaction. Interestingly, only this channel is present (of comparable energetic importance) in the case of silver site whereas the channel supporting backdonation is missing (below assumed threshold). Therefore, as well formaldehyde coordination as carbonyl bond activation are less efficient for Ag(I) site in zeolite than for free Ag^+ cation.

4. Conclusions

In this work adsorption and activation of formaldehyde molecule by copper and silver sites in ZSM-5 was studied by combined QM/MM methodology, enriched by the results of ETS-NOCV analysis decomposing the deformation density into independent density flow channels. The analysis confirmed intuitive view that the bonding of formaldehyde by the cationic site has distinct character from previously studied hydrocarbons bound via double bond according to the well known π-complexation mechanism. Formaldehyde becomes ligated through the carbonyl oxygen as well to free Cu^+ or Ag^+ cations as to cationic M(I) sites in MFI. Bonding mechanism may be described in terms of two density transfer processes: lone pair donation from electron free pair on carbonyl oxygen to the metal and π^*-backdonation from metal d_π orbitals to antibonding orbital of CO. The former one is responsible for the formation of coordination bond in compliance with the intuitive picture while the latter one brings about the activation of carbonyl bond.

Cu(I) site is effectively more efficient than Ag(I) regarding the two types of electronic interaction due to both better intrinsic properties as an electron donor and more efficient cooperation with the framework. Moreover, embedding the cation in MFI framework yields various, partly opposite consequences for Cu^+ or Ag^+. Zeolitic environment is shown to weaken the bond between formaldehyde and M(I) with respect to free cations for both metals but, quite interestingly, π^*-backdonation becomes enhanced in the case of copper while in the case of silver π^*-backdonation becomes diminished. Therefore it seems clear that the net charge density flow is composed of various independent electronic processes and thus cannot fully disclose underlying mechanisms and physical processes accompanying adsorption. In the case of realistic models of active sites it is the ETS-NOCV analysis that helps to separate independent electronic contributions and to rationalize differences in activation properties of M(I) sites relating them to electronic interaction with zeolitic environment.

Calculated red-shifts of C═O stretching frequencies in formaldehyde adsorbed on Cu(I) and Ag(I) sites agree well with the IR-measured ones and correlate with the degree of π^*-backdonation which rationalizes as well very good performance of Cu(I) site compared to Ag(I) as the role of zeolitic framework in modifying exchanged cation properties.

Acknowledgements

This study was sponsored by the Ministry of Science and Education Grant No. N204 1518 36; the work was performed within cooperation partly supported by the IDECAT Network of Excellence.

References

[1] M. Iwamoto, H. Furokawa, Y. Mine, F. Lemura, S. Mikuriya, S. Kagawa, J. Chem. Soc., Chem. Commun. (1986) 1272.
[2] M. Iwamoto, S. Yakoo, K. Sakai, S. Kagawa, Chem. Soc. Faraday Trans. 77 (1981) 1629.
[3] J. Datka, E. Kukulska-Zajac, J. Phys. Chem. B 108 (2004) 17760.
[4] G. Hübner, G. Rauhut, H. Stoll, E. Roduner, Phys. Chem. Chem. Phys. 4 (2002) 3112.
[5] J. Datka, E. Kukulska-Zając, P. Kozyra, J. Mol. Struct. 794 (2006) 261.
[6] E. Broclawik, P. Rejmak, P. Kozyra, J. Datka, Catal. Today 114 (2006) 162.
[7] J. Datka, E. Kukulska-Zając, W. Kobyzewa, Catal. Today 101 (2005) 123.
[8] G. Hübner, G. Rauhut, H. Stoll, E. Roduner, J. Phys. Chem. B 107 (2003) 8568.
[9] E. Kukulska-Zając, P. Kozyra, J. Datka, J. Appl. Catal. A 307 (2006) 46.
[10] P. Kozyra, J. Załucka, M. Mitoraj, E. Brocławik, J. Datka, Catal. Lett. 126 (2008) 241.
[11] J. Datka, P. Kozyra, E. Kukulska-Zając, W. Kobyzewa, Catal. Today 101 (2005) 117.
[12] E. Kukulska-Zajac, J. Datka, J. Phys. Chem. C (2007) 3471.
[13] E. Kukulska-Zając, J. Datka, J. Micropor. Mesopor. Mater. 109 (2008) 49.
[14] E. Brocławik, P. Kozyra, J. Datka, C. R. Chimie 8 (2005) 491.
[15] J. Datka, E. Brocławik, P. Kozyra, E. Kukulska-Zając, D. Bartula, M. Szutiak, Stud. Surf. Sci. Catal. 154 C (2004) 2151.
[16] J. Załucka, P. Kozyra, M. Mitoraj, E. Brocławik, J. Datka, Pol. J. Chem. 81 (2008) 1802.
[17] J. Załucka, P. Kozyra, M. Mitoraj, E. Brocławik, J. Datka, Stud. Surf. Sci. Catal. 174A (2008) 709.
[18] E. Broclawik, J. Załucka, P. Kozyra, M. Mitoraj, J. Datka, J. Phys. Chem. C 114 (2010) 9808.
[19] T. Ziegler, A. Rauk, Inorg. Chem. 18 (1979) 1755.
[20] T. Ziegler, A. Rauk, Theor. Chim. Acta 46 (1977) 1.
[21] M. Mitoraj, A. Michalak, J. Mol. Model. 13 (2007) 347.
[22] A. Michalak, M. Mitoraj, T. Ziegler, J. Phys. Chem. A 112 (2008) 1933.
[23] M. Mitoraj, A. Michalak, Organometallics 26 (2007) 6576.
[24] P. Rejmak, M. Mitoraj, E. Broclawik, Phys. Chem. Chem. Phys. 12 (2010) 2321.
[25] R. Ahlrichs, M. Bär, M. Häser, H. Horn, C.M. Kölmel, Chem. Phys. Lett. 162 (1989) 165.
[26] J.D. Gale, J. Chem. Soc., Faraday Trans. 93 (1997) 629.
[27] M. Sierka, J. Sauer, J. Chem. Phys. 112 (2000) 6983.
[28] (a) A.D. Becke, Phys. Rev. A 38 (1988) 3098;
(b) C. Lee, W. Yang, R.G. Parr, Phys. Rev. B 37 (1998) 785;
(c) A.D Becke, J. Chem. Phys. 98 (1993) 5648.
[29] J.P. Perdew, K. Burke, M. Ernzerhof, Phys. Rev. Lett. 77 (1996) 3865.
[30] B.G. Dick, A.W. Overhauser, Phys. Rev. 112 (1958) 90.
[31] M. Sierka, J. Sauer, Faraday Discuss. 106 (1997) 41.
[32] D. Nachtigallová, P. Nachtigall, M. Sierka, J. Sauer, Phys. Chem. Chem. Phys. 1 (1999) 2019.
[33] P. Dauber-Osguthorpe, V.A. Roberts, D.J. Osguthorpe, J. Wolff, M. Genest, A.T. Hagler, Prot. Struct. Funct. Genet. 4 (1988) 31.
[34] B.A. De Moor, M.-F. Reyniers, M. Sierka, J. Sauer, G.B. Marin, J. Phys. Chem. C 112 (2008) 11796 (supporting info).
[35] ADF2009.01, SCM, Theoretical Chemistry, Vrije Universiteit, Amsterdam, The Netherlands. http://www.scm.com.
[36] A. Michalak, R.L. DeKock, T. Ziegler, J. Phys. Chem. A 112 (2008) 7256.

[37] M. Mitoraj, A. Michalak, J. Mol. Model. 14 (2008) 681.
[38] M. Mitoraj, H. Zhu, A. Michalak, T. Ziegler, Int. J. Quant. Chem. 109 (2009) 3379.
[39] M. Srebro, M. Mitoraj, Organometallics 28 (2009) 3650.
[40] M. Srebro, A. Michalak, Inorg. Chem. 48 (2009) 5361.
[41] M. Radon, Theor. Chem. Acc. 120 (2008) 337.
[42] R.F. Nalewajski, J. Korchowiec, A. Michalak, Reactivity criteria in charge sensitivity analysis, in: R.F. Nalewajski (Ed.), Topics in Current Chemistry, vol. 183, Density Functional Theory—Theory of Chemical Reactivity, Springer-Verlag, Heidelberg, 1996, p. 25.
[43] M. Mitoraj, A. Michalak, T. Ziegler, J. Chem. Theory Comput. 5 (2009) 962.
[44] M. Mitoraj, A. Michalak, T. Ziegler, Organometallics 28 (2009) 3727.